Inhomogenous Dielectric Metamaterials with Space-Variant Polarizability

Uriel Levy,[1,*] Maxim Abashin,[1] Kazuhiro Ikeda,[1] Ashok Krishnamoorthy,[2] John Cunningham,[2] and Yeshaiahu Fainman[1]

[1]*Dept. of Electrical and Computer Engineering, University of California, San Diego, 9500 Gilman Drive, La Jolla California, 92093-0407, USA*

[2]*Sun Microsystems Physical Sciences Center, 9515 Towne Centre Drive, Mailstop USAN10-107, San Diego, CA 92121, USA*

(Received 4 December 2006; published 13 June 2007)

We experimentally demonstrate for the first time the focusing of optical beams within an inhomogeneous dielectric metamaterial with space-variant polarizability, implemented by etching subwavelength structures into a Silicon slab. Light focusing is obtained by creating an artificial slab material with graded refractive index profile. The local refractive index within the slab is modulated by controlling the duty cycle of the subwavelength structures. The demonstrated metamaterial based component can be integrated with various other building blocks towards the realization of devices and systems in free space optics on a chip configuration.

DOI: 10.1103/PhysRevLett.98.243901 PACS numbers: 42.70.−a, 41.85.Ew, 42.82.Et, 78.67.−n

Introduction.—The field of nanophotonics is finding myriad applications in information technology, health care, lighting, sensing, and national security. The rapid advance in the nanophotonic field is often attributed to the discovery of photonic crystals (PhC) [1–4]. These periodic dielectric structures can be designed to have a photonic band gap, essentially preventing optical fields at the band gap frequency region from propagating within the structure. Allowed states can be generated by introducing defects into the structure, allowing the realization of PhC waveguides [5], ultra small cavities with high quality factor [6], and lasers [7]. The PhC can be also designed to operate outside the region of photonic band gap, realizing devices such as super collimators, super prisms, and super lenses [8–10] through proper design and optimization of Bloch modes. Most of the PhC devices are defined in two dimensions and light is vertically confined by total internal reflection.

An alternative approach is the realization of a system that benefits from devices that exploit the advantages of both continuous free space and discrete guided wave modes. A common example is the propagation of light in a slab waveguide, which supports confinement in the vertical direction and free space propagation in the plane of the slab. We call such a configuration "free space optics on a chip'' (FSOC). This configuration allows light to propagate freely in the slab, while interacting with discrete optical components that are located along the propagation direction. Towards the implementation of practical FSOC devices, one needs to realize typical free space functionalities, e.g., focusing, beam steering, bending, and wavelength selectivity on chip. We implement such functionalities by introducing inhomogeneous dielectric metamaterials with space-variant polarizability into the slab waveguide. These metamaterials, realized by using nanolithography and advanced etching techniques, allow modulating the local effective index of refraction in the plane of the slab.

In this Letter, we provide the first demonstration of our FSOC concept by experimentally realizing a graded index lens implemented by space-variant inhomogeneous metamaterial that locally modulates the effective index of refraction of a slab made of Silicon-On-Insulator (SOI). The effective refractive index of the Silicon (Si) slab is modified by defining and etching patterns that are much smaller than the wavelength of light in the slab. The local effective refractive index can be estimated using effective medium theory (EMT) [11] or more accurately using rigorous coupled wave analysis (assuming slowly varying period) [12]. These methods have been used in the past for synthesis of form birefringent metamaterials for operation in free space [13] and in guided wave [14] regimes. Notice that the interaction length in the guided wave configuration is limited only by geometrical considerations. In general, this approach allows for optimization of the SOI slab with space-variant (i.e., spatially inhomogeneous), arbitrarily defined effective refractive index profile across not only the transverse but also along the propagation direction. In this Letter, we demonstrate an example of a spatially inhomogeneous slab implementing lens functionality by creating a quadratic effective index of refraction in the transverse direction of the slab.

The metamaterial-based focusing component, schematically depicted in Fig. 1, is realized by lithographically defining and etching subwavelength features into a high refractive index slab waveguide, modifying its local effective index of refraction. Because of the space-variant nature of the structure, Bloch theorem cannot be applied in its direct form. Instead, the local effective refractive index for the out-of-plane (TM) polarization is estimated by using the second order EMT:

$$(n_{\mathrm{Eff}}^{(2)})^2 = (n_{\mathrm{Eff}}^{(0)})^2 + \frac{1}{3}\left[\frac{\Lambda}{\lambda}\pi f(1-f)(n_{e\mathrm{Si}}^2 - n_{\mathrm{cl1}}^2)\right]^2 \quad (1)$$

where Λ is the period of the subwavelength grating, λ is the optical wavelength in vacuum, f is the local duty cycle

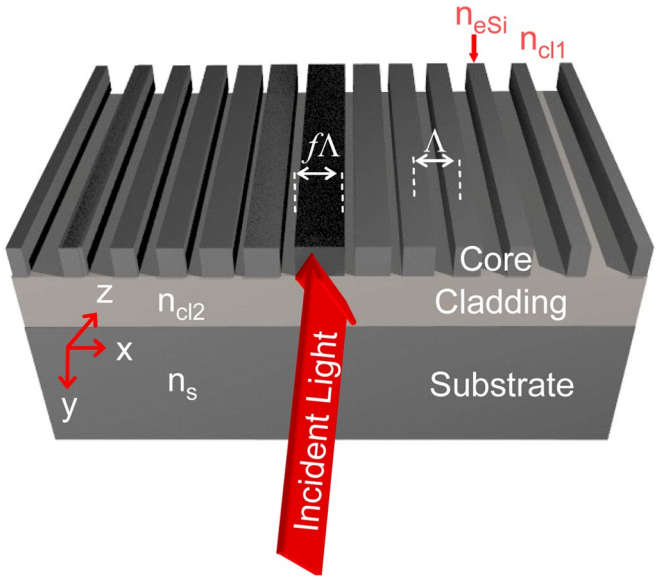

FIG. 1 (color online). Schematic drawing showing the geometry of the slab lens. Λ is the period of the grating, f is the local duty cycle, $n_{e\mathrm{Si}}$, n_{cl1}, n_{cl2}, and n_s are the effective refractive index of the Si slab, the upper (typically $n_{\mathrm{cl1}} = 1$) and lower cladding, and the substrate, respectively. The thick arrow shows the light propagation direction (along the z-axis).

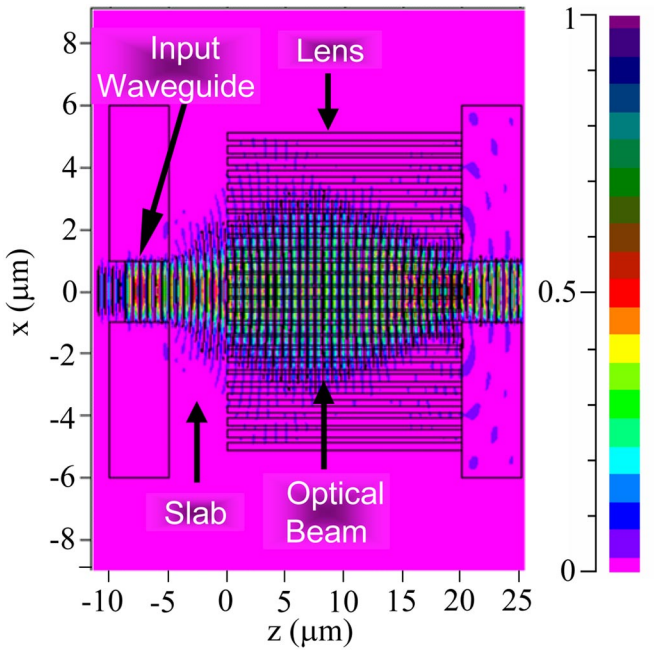

FIG. 2 (color online). Device layout consisting of input ridge waveguide, nonpatterned slab, slab lens, and output ridge waveguide. An overlayed finite difference time domain simulation shows the beam propagation, which is found in good agreement with the approximate design of device layout using effective medium theory. Device layout is also shown. The simulation results clearly show the focusing of light towards the output ridge waveguide.

of the grating, $n_{e\mathrm{Si}}$ is the effective refractive index of the nonpatterned slab, n_{cl1} is the refractive index of the surrounding medium (typically air), and $[n_{\mathrm{Eff}}^{(0)}]^2 = f n_{e\mathrm{Si}}^2 + (1-f) n_{\mathrm{cl1}}^2$. Equation (1) shows that the effective refractive index profile can be synthesized in the transverse, x direction, by locally modulating the duty cycle $f = f(x)$. To demonstrate the concept, we choose to realize a graded index slab lens. Thus, we are looking for a solution, $f(x)$, that would create a material with quadratic refractive index profile, i.e., $n(x) = n_0(1 - 0.5\alpha x^2)$, where n_0 and α are constants representing the maximal effective index and the gradient strength, respectively. The solution is obtained by replacing the left-hand side of Eq. (1) with the quadratic refractive index term and solving the resultant equation for $f(x)$. It should be noted that the device can be also designed to operate under TE-polarized light illumination. In such a case, the EMT equation for TE-polarized light should be used, and the appropriate effective index of the slab should be taken into account.

To validate our approach, we designed and fabricated an inhomogeneous dielectric metamaterial-based graded index slab lens that focuses light into a 2-μm wide Si ridge waveguide. We used SOI geometry with a Si slab thickness of 250 nm and an oxide thickness of 3 μm. The layout of the sample and the modeling results are shown in Fig. 2. Light emerges from a 2-μm wide input ridge waveguide into a 5-μm long section of nonpatterned slab, experiencing free space propagation in the transverse direction while being confined in the vertical direction. The beam expands in the transverse direction due to diffraction effects before entering the slab lens designed to refocus the optical field into the output waveguide. The effective refractive index of the slab of Si with $n_{\mathrm{Si}} = 3.47$ $n_{\mathrm{cl1}} = 1$ and $n_{\mathrm{cl2}} = 1.45$ for TM polarization is about 2.3. A grating period of 400 nm is chosen to assure the validity of the effective medium approximation on one hand, and to avoid the need for fabricating ultra small features. The modulation of the duty cycle is constrained in its upper and lower bounds by the nanofabrication process and by light guiding requirements in the vertical direction of the slab, respectively. For compatibility with CMOS fabrication, the minimal air gap is chosen to be 100 nm, imposing a maximal duty cycle of 75%. Using Eq. (1) and the 75% grating duty cycle, we estimate maximal refractive index of $n_0 = 2.1$. The lower bound on the duty cycle of about 35% is determined by requiring that the local effective refractive index of the patterned slab remains higher than the refractive index of the oxide cladding layer (n_{cl2}). The width of the slab lens, 10 μm, is determined from the expansion of the optical field in the transverse direction of the nonpatterned slab section. This expansion is estimated with Gaussian optics calculation to be about 6 μm at the input facet of the slab lens. These parameters determine that the maximal parabolic factor (α) is about 0.015. Using Gaussian optics, we estimate that after propagation of about 20 μm inside the slab lens, a new Gaussian beam

waist of about 2 μm diameter is obtained. To test this somewhat heuristic calculation, we conduct a finite difference time domain (FDTD) simulation. The results, also shown in Fig. 2, agree very well with the theoretical prediction.

Fabrication of the metamaterial based graded index lens consists of patterning the device using electron beam lithography followed by reactive ion etching with Chlorine based chemistry. An SEM micrograph showing the layout of the entire fabricated device is depicted in Fig. 3(a). A slanted view of a magnified portion of the device is shown in Fig. 3(b).

We estimated the accuracy of the fabricated structure by acquiring a sequence of magnified top-view SEM images from which we estimated the local duty cycle. In general, the obtained local duty cycle was slightly larger than the designed one. This was particularly noticeable around the central portion of the lens. For example, the central airgap was only ~50–60 nm wide, as oppose to the designed value of 100 nm. We believe that this deviation can be attributed mostly to the proximity effect. Proximity correction [15] can be applied to further improve the fabrication process.

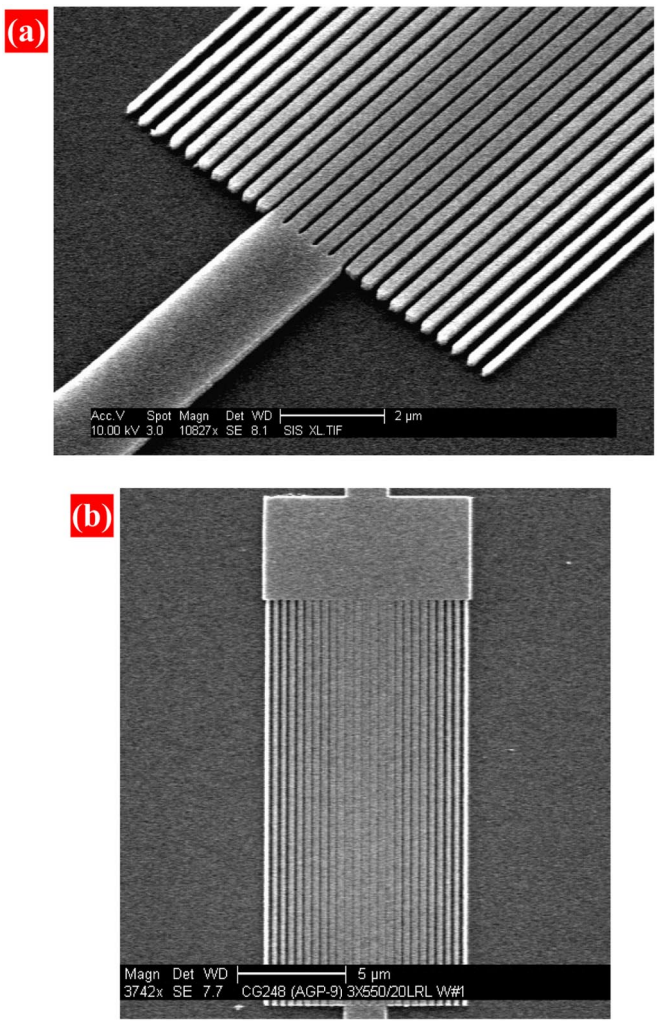

FIG. 3 (color online). Scanning electron micrograph showing the fabricated device: (a) a top view of the entire structure. (b) a magnified slanted view showing part of the slab lens and the output waveguide.

To better understand the effect of structural deviation on the propagation of light within the device, we conducted an additional FDTD simulation taking into account the geometry of the fabricated structure. The result, depicted in Fig. 4, shows that focusing occurred within the structure, about 6 μm before the output. The "over focusing" effect is expected, as the higher values of duty cycle around the central section create an effective material with larger quadratic parameter α as compared to that of the designed one.

Typically, characterization of nanophotonic devices is performed by analyzing the light intensity measured at the output of the device. Unfortunately, this approach lacks the ability to probe the amplitude and, even more importantly, the phase profile of the optical beam as it propagates within the structure. To overcome this deficiency, the fabricated samples are characterized using our heterodyne near field scanning optical microscope (H-NSOM) [16], capable of measuring both amplitude and phase of the propagating optical field with a resolution of about 100 nm. The H-NSOM is ideal for characterization of our component because it allows direct observation of the curvature of the spatial phase front of the field propagating in the slab lens. Figure 5 shows the measured amplitude and phase of

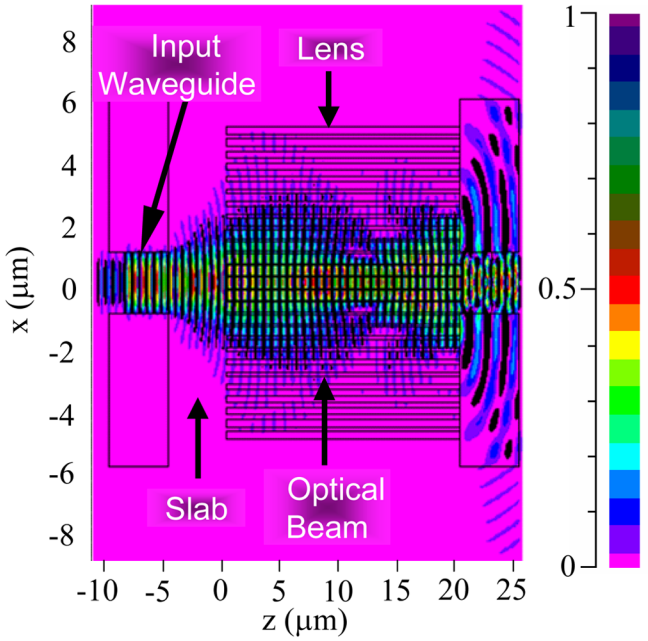

FIG. 4 (color online). Finite difference time domain simulation shows the beam propagation, within the device, where the deviation of the fabricated structure from the design is taken into account. Result shows that focusing occurs about 5 mm before the output waveguide.

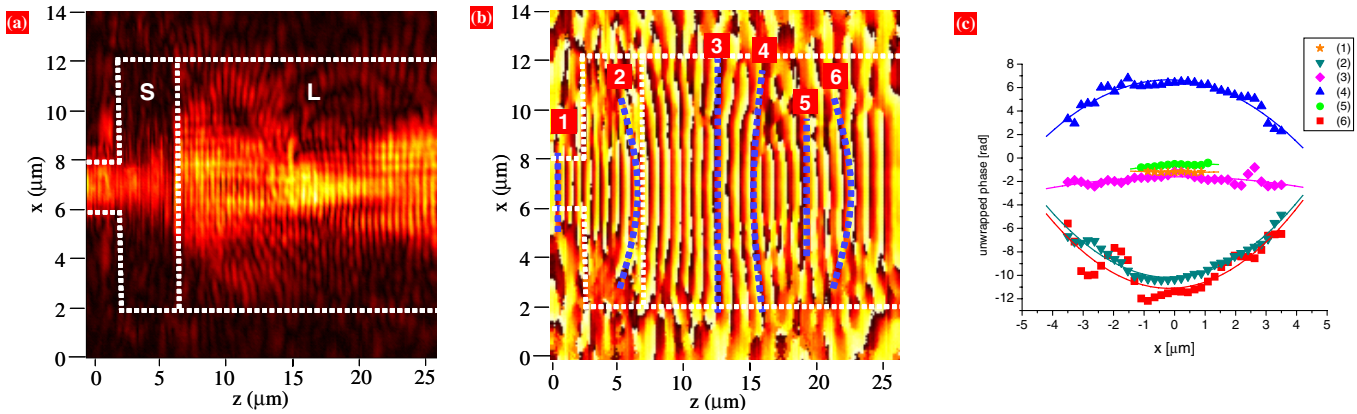

FIG. 5 (color online). Experimental results obtained with the Heterodyne Near field Scanning Optical Microscope (H-NSOM). (a) The amplitude and (b) the phase of the optical field in the region that includes the input waveguide, the nonpatterned slab (S), and large portion of the slab lens section (L). The dashed vertical lines mark the boundaries between the various sections. Light is propagating from left to right. (c) Cross sections showing phase profile at several planes along the device. The planes are marked in Fig. 5b.

the optical field propagating through the device at a wavelength of $\lambda = 1550$ nm. Figure 5(a) shows the amplitude of the optical field in the region that includes the input waveguide, the nonpatterned slab (S), and large portion of the slab lens section (L). The dashed vertical lines mark the boundaries between the various sections of the device. Light propagates from left to right. Figure 5(b) shows the measured phase in the same region. Figure 5(c) shows several cross sections of the phase front calculated from Fig. 5(b) at several planes along the z-axis. The obtained results clearly show the expanding of the optical beam in the region of the slab. As expected, the phase front is diverging in this section. As the beam enters the metamaterial, the curvature of the phase front is gradually decreasing and becomes planar after about 5 μm propagation in the slab. Then, the phase front begins to converge towards the focus. As anticipated from Fig. 4, the new focus is generated slightly before the output waveguide. This can be observed both from the phase image, showing a planar phase profile about 6 μm before the end of the slab lens [Fig. 5(b) and 5(c)], and from the amplitude image, showing a strong peak at the same location [Fig. 5(a)]. As the beam continues to propagate, the phase front starts to diverge again, and the optical beam expands.

In conclusion, we investigated experimentally a novel metamaterial based graded index slab lens device which is the first step towards the realization of our proposed FSOC concept. Our Heterodyne-based near field measurements clearly demonstrate the focusing effect. This experimental demonstration opens new possibilities in the field of on chip integrated photonic devices, as the demonstrated component can be integrated with other building blocks to create future devices and systems based on the concept of FSOC. We believe that this new concept may become essential for applications such as optical interconnections, information processing, spectroscopy, and sensing on a chip.

This work was partially supported by NSF, AFOSR, and DARPA.

*Present address: Department of Applied Physics, the Benin School of Engineering and Computer Science, the Hebrew University of Jerusalem, Jerusalem, 91904 Israel. ulevy@cc.huji.ac.il

[1] E. Yablonovitch, Phys. Rev. Lett. **58**, 2059 (1987).
[2] S. John, Phys. Rev. Lett. **58**, 2486 (1987).
[3] J. D. Joannopoulos, R. D. Meade, and J. N. Winn, *Photonic Crystals* (Princeton University Press, Princeton, NJ, 1995).
[4] T. F. Krauss, R. M. De La Rue, and S. Brand, Nature (London) **383**, 699 (1996).
[5] M. Loncar *et al.*, Appl. Phys. Lett. **77**, 1937 (2000).
[6] Y. Akahane *et al.*, Nature (London) **425**, 944 (2003).
[7] O. Painter *et al.*, Science **284**, 1819 (1999).
[8] H. Kosaka *et al.*, Appl. Phys. Lett. **74**, 1212 (1999).
[9] H. Kosaka *et al.*, J. Lightwave Technol. **17**, 2032 (1999).
[10] C. Luo *et al.*, Phys. Rev. B **68**, 045115 (2003).
[11] S. M. Rytov, Sov. Phys. JETP **2**, 466 (1956).
[12] I. Richter *et al.*, Appl. Opt. **34**, 2421 (1995).
[13] F. Xu *et al.*, Opt. Lett. **20**, 2457 (1995).
[14] U. Levy *et al.*, J. Opt. Soc. Am. A **22**, 724 (2005).
[15] M. Parikh, J. Appl. Phys. **50**, 4371 (1979).
[16] A. Nesci and Y. Fainman, in *Wave Optics and Photonic Devices for Optical Information Processing II*, edited by P. Ambs and F. R. Beyette, Jr., Proc. SPIE Int. Soc. Opt. Eng. Vol. 5181 (SPIE-Internation Society for Optical Engineering, Bellingham, WA, 2003), p. 62.